

Article

Not peer-reviewed version

Four Petal-Specific TPS Drive Nocturnal Terpene Scent in *Jasminum sambac*

[Yuan Yuan](#), [Li Hu](#), [Xian He](#), [Jinan Li](#), [Chao Wan](#), [Yue Zhang](#), Yuting Wang, [Wei Wang](#), [Binghua Wu](#)*

Posted Date: 24 November 2025

doi: 10.20944/preprints202511.1707.v1

Keywords: *Jasminum sambac*; floral scent; monoterpenoids; sesquiterpenoids; terpene synthase; linalool; nerolidol; farnesol; cadinol



Preprints.org is a free multidisciplinary platform providing preprint service that is dedicated to making early versions of research outputs permanently available and citable. Preprints posted at Preprints.org appear in Web of Science, Crossref, Google Scholar, Scilit, Europe PMC.

Copyright: This open access article is published under a [Creative Commons CC BY 4.0 license](#), which permit the free download, distribution, and reuse, provided that the author and preprint are cited in any reuse.

Disclaimer/Publisher's Note: The statements, opinions, and data contained in all publications are solely those of the individual author(s) and contributor(s) and not of MDPI and/or the editor(s). MDPI and/or the editor(s) disclaim responsibility for any injury to people or property resulting from any ideas, methods, instructions, or products referred to in the content.

Article

Four Petal-Specific TPS Drive Nocturnal Terpene scent in *Jasminum sambac*

Yuan Yuan, Li Hu, Xian He, Jinan Li, Chao Wan, Yue Zhang, Yuting Wang, Wei Wang and Binghua Wu *

College of Horticulture, Fujian Agriculture and Forestry University, Fuzhou, Fujian 350002, China

* Correspondence: binghua.wu@fafu.edu.cn; Tel.: +86 (0) 188 50498434

Abstract

Floral volatile terpenoids are known to play important roles in plant pollination biology by attracting animal pollinators and repelling antagonists, as well as enhancing resistance to potential microbial pathogens. Terpeneoid blend emitted by a flower is usually plant-lineage specific and mostly determined by a set of versatile terpene synthases (TPSs) which catalyze the final step of diverse terpeneoid synthesis. The strongly scented flower of *Jasminum sambac* emits linalool and α -farnesene dominating the nocturnal floral VOC, yet the corresponding TPSs have not been identified. Here, we show that four TPS enzymes are responsible for the synthesis of the mixtures of volatile terpenoids in the flower, based on their highly-correlated and almost-exclusive expression in the petal, and on their enzymatic characterizations *in vitro* and in *Nicotiana benthamiana*. JsTPS01 (TPS-a) acts as a sesquiterpene synthase, producing τ -cadinol in yeast at levels that mirror its rhythmic expression in petals. JsTPS02 (TPS-b) carries a plastid-transit peptide, localizes to chloroplasts/plastids, and converts GPP to linalool with high affinity ($K_m = 28.2 \pm 3.4 \mu\text{M}$). JsTPS03 is a TPS-b clade member that is able to convert FPP to farnesol with a K_m of $14.4 \pm 5.9 \mu\text{M}$ in an *in vitro* assay using isolated yeast vehicles. JsTPS04 (TPS-e/f) exhibits dual targeting—cytosolic in *Arabidopsis* protoplasts but plastidic in *J. sambac* petals—and functions as a bifunctional mono-/sesqui-TPS, forming linalool from GPP ($K_m = 2.5 \pm 0.3 \mu\text{M}$) and trans-nerolidol from FPP ($K_m = 7.6 \pm 0.6 \mu\text{M}$). Transient expression in *Nicotiana benthamiana* leaves further confirmed its *in-planta* linalool production. collectively, we identified four preferentially expressed terpene synthases contribute to linalool, τ -cadinol, trans-nerolidol, and farnesol in *Jasminum sambac*.

Keywords: *Jasminum sambac*; floral scent; monoterpenoids; sesquiterpenoids; terpene synthase; linalool; nerolidol; farnesol; cadinol

1. Introduction

Plant utilizes diverse 'secondary' compounds made from its specialized metabolisms for interactions with the surrounding abiotic or biotic factors [1]. The ecological and/or physiological roles of plant specialized metabolites are often lineage-specific or evolutionary convergent, with well-known examples in herbivore defense [2], UV protection [3] or pollinator attraction [4,5]. An estimation on the number of these specialized compounds across the plant kingdom suggests a range in hundreds of thousands [6] and, the enzymes responsible for making the chemical diversity are known to possess lower catalytic efficiency but remarkable substrate or product promiscuity [7–9].

Terpenoids or isoprenoids are one of the most diverse classes of such compounds, the final step in synthesis of which is mainly catalyzed by two groups of closely related enzymes called prenyl transferases (PTs) and terpene synthase (TPSs) [10]. Precursors of the reactions are the two isomeric 5-carbon (C5) building blocks isopentenyl diphosphate (IPP) and dimethylallyl diphosphate (DMAPP), as well as their condensed derivatives geranyl diphosphate (GPP, C10), neryl diphosphate (NPP, C10), farnesyl diphosphate (FPP, C15) and geranylgeranyl diphosphate (GGPP, C20) [11,12]. In plants, IPP and DMAPP are generated via two independent and compartmentally separated

pathways, the acetyl-CoA derived cytosolic mevalonate (MVA) pathway and the pyruvate derived plastidial 2-C-methyl-D-erythritol-4-phosphate (MEP) pathway [13]. While PTs usually work in condensation of the two C5 blocks [14], or in generation of longer-chain polyisoprenoids via sequential head-to-tail additions of IPP [15], TPSs catalyze the final production of the many structurally distinct isoprenoid molecules which may be modified, simultaneously or subsequently, by the cytochrome P450 monooxygenase (P450) enzymes to give rise to the diversity of nature terpenoid compounds [16–18]. Many of the lower molecular weight and high melting point acyclic or cyclic terpenoids, mostly the C10 monoterpenoids and the C15 sesquiterpenoids are volatile organic compounds (VOC) that function essentially as pollinator or seed-disperser attractants and defense arsenals [19,20]. Recent studies on the structural and functional divergence of the TPS family has highlighted the evolutionary importance of terpenoids in mediating plant-plant and plant-microbe interaction that affects plant fitness and adaptation [21–25].

Most fragrant flowers typically emit a mixture of between 20 and 60 different compounds derived from limited metabolic pathways including the terpenoid, lipoxygenase and phenylpropanoid/benzenoid pathways. While volatile fatty acid derivatives and phenylpropanoids/benzenoids are commonly found in floral scents, terpenoids constitute the largest class of floral volatiles [26]. It is suggested that floral scent is an important trait of pollination syndromes that may impact plant reproduction strategy and contribute to reproductive isolation as well, and that either 'structural' or 'regulatory' genes responsible for the production of the fragrant compounds are under evolutionary selection imposed by both mutualists and antagonists [5,27–29]. In the model plant *Arabidopsis thaliana*, the genome encodes 32 TPS full-length genes among which more than half have been functionally investigated including 4 flower-specific terpene synthase (TPS11,14, 21 and 24) genes that together with the widely-expressed TPS03 and TPS10 contribute to a mix of emitted monoterpenes and sesquiterpenes in the flower, despite the low level of the emission rate [30,31]. Interestingly, the same set of floral terpenoids is similarly produced among 37 *Arabidopsis* ecotypes, indicating an inherited role in reproduction fitness or for pollination strategy of this species [32]. The second most extensively studied plant species for the TPS functionality is the cultivated tomato (*Solanum lycopersicum*), the genome of which contains at least 52 loci with 34 putative functional TPS genes, representing all the seven clades of the TPS family [25,33]. However, tomato flowers as well as the *Arabidopsis*, are usually wind-pollinated with occasional aid by insects like bumble bees. The expression of several non-exclusive floral TPSs is consistent with the mild release of volatile mono- and sesquiterpenes [25,33]. For plant species with strongly scented flowers, such as *Clarkia breweri*, *Antirrhinum majus* and several orchid plants, knowledge about the composition of specific fragrant bouquet, the genes underpinning the biosynthetic regulation, as well as the eco-evolutionary significance of the floral scent from particular plant lineages are increasingly documented [20,34–40]. Despite the great progresses made, however, much less investigation has been reported in many other fragrant plants, especially those without handful genetic tools [41].

Jasminum sambac (L.) Aiton, a nocturnal anthesis species from the olive family (Oleaceae), is an evergreen shrub or vine native to India or Southeast Asia and cultivated worldwide for the showy and exceptionally fragrant flowers. Most *Jasminum* species are distylous in floral morphology [42] and the cultivated plants are usually clonally propagated that may also be due to the lack of natural seed-setting [43]. In Asia the flowers are used for essential oil industry and for scented tea production. The closely related species in the Genus including *J. grandiflorum*, *J. asteroides* and *J. auriculatum* are also used for the same purpose and their floral VOCs constitute a highly characteristic proportion of benzyl acetate, linalool, and α -farnesene, with quantitative variation of other minor terpenoids and phenylpropanoids/benzenoids among them [44–50]. In one experiment, enzyme activities of several biosynthesis enzymes including terpene synthase were determined using crude petal extract, roughly correlating to the VOC emission rate [45]. However, the corresponding genes encoding such enzymes were still elusive. In recent years, genome data for different jasmine cultivars have been reported successively [48–54], along with analyses of the terpene synthase (TPS) gene family [48,53,55]. A TPS

responsible for synthesizing β -ocimene has also been described [48]; however, the TPS involved in the biosynthesis of linalool—a dominant terpene aroma compound—has not yet been reported.

Here, we showed that four highly expressed flower-specific TPS were responsible for the biosynthesis of the floral monoterpenoids and sesquiterpenoids in *J. sambac*. Specifically, the most strongly expressing *JsTPS04* produces both the monoterpene linalool and the sesquiterpene tansnerolidol, *JsTPS03* convert FPP to farnesol, *JsTPS02* is dedicated to linalool formation, and *JsTPS01* generates the sesquiterpene τ -cadinol in yeast. It remains to be determined how these genes are regulated and the relevance to the pollination syndromes.

2. Materials and Methods

Plant materials and growth conditions

Three-year old plants of double petal *J. sambac* were obtained by clonal propagation in a nursery and grown in pots of $\varnothing 30 \times 40$ cm, filled with peat, perlite and vermiculite in a ratio of 7:0.5:3. In their third year, plants were moved to a climate room with a photoperiod of 16 h/8 h (light/dark), a temperature regime at 26/22 °C (light/dark) and a constant relative humidity at 70%, and maintained with regulatory watering.

During the experiments, 20 plants were used in headspace determination. Another 40 plants were used for petal extraction of VOC, analysis of gene expression and protoplast isolation. Since *J. sambac* anthesis started at ~18:00 of the day, all mature flower buds (approximately 1-2 cm in wide) were labeled with a plastic tag in the afternoon and the life-time of the flowers were followed and sampled accordingly. For repeated experiments, we usually carried out pruning on all plants after flowering to maintain a unified growth status and plant height.

Plants of *A. thaliana* (Columbia-0) and *N. benthamiana* were grown in a climate room at 24 °C/20 °C (light/dark) with a photoperiod of 16 h/8 h (light/dark).

Headspace and petal extract volatile compound collection

A simple headspace measurement was employed to monitor the VOC during the flowering lifetime in a 2-h-interval starting from 17:00 until the next 48 h, in which one removed flower at each sampling time was enclosed in a Perkin Elmer sample vial (20 ml) and kept at 50°C for 25 min before automatic injection (1 μ L of the headspace) into the GC-MS. The determination was conducted in triplicates and the experiment repeated three times.

For VOC analysis in petal extracts, collected petals were ground into fine powders in liquid nitrogen and ~ 0.5 g of these were transferred to a 5 mL glass vial. 1.0 mL n-hexane (cat.nr. 1.04391.4008, Merck KGaA, Darmstadt, Germany) was added to extract the organic compounds for 24 hours in room temperature. After centrifugation at 2500 \times g for 10 min at 4 °C, the supernatants were passed through a 0.22 μ m membrane filter, collected and subjected to GC-MS. The experiments were repeated three times.

For quantification, peak area was calibrated using an 5 ng· μ L⁻¹ internal standard α -Cedrene (cat. Nr. 22133, Merck KGaA, Darmstadt, Germany). (supplementary data set 1).

RNA extraction and reverse transcription

Flowers were collected at continued time-points of every two hours during flowering starting from 17:00 RNA, similar to the sampling for scent determination. Petals were removed and frozen in liquid nitrogen immediately after flower collections. About 100 mg liquid-nitrogen-ground-powder of petal was used for RNA extraction with the TransZol Up Plus RNA Kit (TransGen Biotech, Shanghai, China), per manufacturer's standard protocol. The purity and concentration of RNA were assessed using a Nanodrop 1000 spectrophotometer (Thermo Scientific, Waltham, MA, USA). Approximately 1 μ g total RNA was used for cDNA synthesis in a final reaction volume of 20 μ l containing Oligo d(T)18 primers and the transcript[®] RT/RI Enzyme Transcriptase (TransGen Biotech) according to the manufacturer's specifications.

Transcriptome data mining, full-length cDNA cloning, plasmid construction and sequence analysis

Three replicates of flower at 17:00 (F1), 01:00 (the following day, F2), 09:00 (the following day, F3) and young stem (S) and leaf (L) sample were used to extract total RNA. A total of 15 libraries (F1, F2, F3, L, S, three biological duplicates) were constructed and sequenced with the Illumina NovaSeq 6000 sequencer (2 × 150 bp read length). For raw data, FastQC (version 0.11.5) was used for quality control and the Fastp (version 0.20.0) was used for filtering. The filtered clean reads were then independently mapped to the double petal Jasmine genome (GWHBFHJ000000000) by HISAT2 (v2.1.0) for subsequent different analyses [56]. The expression level of each transcript was calculated by the Transcripts per million reads (TPM) was used to determine each transcript's expression level, and genes were classified as differentially expressed genes (DEGs) if $|\log_2 FC| \geq 1$ and adjusted Pvalue ≤ 0.05 . Kyoto Encyclopedia of Genes and Genomes (KEGG) enrichment analysis of DEGs was performed by clusterProfiler R software (v4.0) [57]. To identified TPS related sequences in the flower and leaf transcriptomes, local BLAST search was conducted with known TPSs from other plants, resulting in 34 original sequences, that were further reduced to a set of 4 genes by screening for genes that are highly expressed in flowers but lowly expressed in leaves. (Tab S1) Primers for quantitative RT-PCR were designed accordingly, using Primer3 plus at <http://www.bioinformatics.nl/cgi-bin/primer3plus/> with default setting. The primers are listed in Tab. S2.

For CDS cloning of four TPS genes, Total RNA was isolated using a TransZol Up Plus RNA Kit (TransGen Biotech, Shanghai, China). Synthesis of cDNA was conducted in a 20 μ L reaction containing Oligo d(T)18 primers and the transcript[®] RT/RI Enzyme Transcriptase (TransGen Biotech) using approximately 1 μ g total RNA as templates following the manufacturer's instruction. The full-length JsTPS cDNA were PCR amplified using designed primers (Tab. S2) and then sub-cloned into the pENTR[™]/D-TOPO[®] (Thermo Fisher Scientific, Shanghai, China) and subsequently into a binary vector pK7FWG2 [58] using LR reaction (ThermoFisher, Shanghai, China) yielding pK7-JsTPS01/02/03/04-GFP, respectively. This Gateway cloning strategy resulted in a 16-amino-acid-likier 'KGGRA DPAFL YKVVV I S' between the JsTPS's C-terminal and the GFP. A control vector pK7-GFP expressing the GFP alone was described previously [59]. All constructs had been verified by Sanger sequencing.

For sequence alignment and phylogenetic tree constructions, the web-based program MUSCLE (<https://www.ebi.ac.uk/Tools/msa/muscle/>) was used with the default parameters. The protein sequences of other TPSs with known functions and/or structures were retrieved from SSWISS/Pro. A Neighbor-Joining tree was constructed using MEGA X ver. 10.1.8 [60] with 1000 bootstrap number and visualized via Figtree ver. 1.4.4. (downloaded from <http://tree.bio.ed.ac.uk/software/figtree/>).

Quantitative real-time PCR analysis

Quantitative RT-PCR was performed on a Roche LightCycler 96, using 1 μ l cDNA in a 20 μ l of reaction mixture containing 10 μ l of 2×TransStart[®] Green qPCR SuperMix (TransGen Biotech), 0.2 μ M of each primer pair (Tab.S1). The relative expression level of target genes was calculated by the 2^{- Δ CT} method [61]. For measurement on petal samples at various time point during flowering, 3-5 flowers from 3 plants were pooled as a biological sample which was determined by at least 3 technical replicates.

Subcellular localization of JsTPS proteins in protoplasts and *N. benthamiana*

The binary vectors pK7-JsTPSs expressing the candidate enzymes in fusion with a C-terminal GFP driven by the cauliflower mosaic virus 35S promoter were used for PEG-mediated transfection of protoplasts isolated from either 5-week-old Arabidopsis rosette leaves or fully-open *Jasminum* petals, as describe elsewhere [62]. After incubation at room temperature for 20~22 h in darkness, the protoplasts were examined under a Leica M205 FA confocal microscope with a filter setting for GFP (excitation at 470/40 nm, emission at 525/50 nm) and for chlorophyll auto-fluorescence (excitation at 545/30 nm, emission at 620/60 nm).

The same set of binary vectors were also used in agoinfiltration-based transient expression in leaves of 4-week-old *N. benthamiana* plants. This was done by growing *Agrobacterium tumefaciens* strain GV3101 harboring the respective vectors to a cell-density of 1 OD_{600nm} and further incubating without shaking at room temperature for 2-3 h after washing and resuspending to a final 0.1 OD_{600nm}

in an infiltration medium (10 mM MES buffered MS with 3 % sucrose and 200 μ m acetosyringone, pH 6.1).

The epidermis was removed from the leaves at 2 days post infiltration for fluorescence observation under the same microscope conditions.

Transient Expression in N. benthamiana and Collection of Emitted Volatiles

Similar to fluorescence observation in *N. benthamiana* leaves transiently expressing the JsTPS-GFP fusions, the infiltrated tobacco plants were maintained in a growth chamber at 22 °C with 16 h light/8 h dark. Two days after infiltration, infected leaves were harvested and leaf disks were cut from the infected area, and ground into fine powder in liquid nitrogen immediately. Approximately 0.5 g of the powder was extracted with 1.5 mL ethyl acetate and the supernatant after centrifugation at 13000 x g for 10 min at 4°C was clarified by passing through a 0.22 μ m filter before subjecting to GC/MS analysis. The leaves infiltrated with an *Agrobacterium* harboring the pK7-GFP vector served as an empty vector (EV) control.

Heterologous Expression in Yeast

The yeast expression vectors were constructed based on the plasmid pDRTxa [63] by ligation of the *Bam*H I and *Sal* I restricted PCR fragments to the same restricted plasmid, respectively. The specific primers could be found in Tab. S2. The yeast strain By4742 was the expression host and transformed via the standard PEG protocol [64]. A single colony of the transformants was grown in 10 mL selection medium (SD-ura) at 28°C overnight with shaking at 200 rpm. This preculture was diluted in a 120 mL SD-ura to an initial OD_{600nm} = 0.2. After the OD_{600nm} reaching 0.8, the excreted products were extracted using solid phase extraction cartridges (Oasis HLB 3cc/60mg from Waters, Shanghai, China), according to the manufacturer's guidelines. After washing and drying, the loaded cartridges were eluted with 2.5 mL ethyl acetate containing 5 ng/ μ L α -cedrene (cat. Nr. 22133 from Sigma-Aldrich, Shanghai, China) as an internal standard and the combined organic phase was dehydrated over Na₂SO₄, concentrated in a stream of nitrogen to dryness and re-dissolved in 200 μ L ethyl acetate before GC-MS analysis. Empty vector-transformed yeast cells were used as mock control (EV).

Recombinant Proteins and In Vitro enzyme assay of four JsTPSs

The cDNA of each JsTPS was amplified with pK7-JsTPSs plasmid as a template and subcloned into pET21HA vector, using *Bam*H I/*Sal* I (Thermo Scientific) restriction sites. The resulting plasmid was introduced into an *E. coli* Rosetta (DE3) (WEIDI, Shanghai). The transformant was grown to an 0.6 OD_{600nm} before induction of protein expression. The recombinant JsTPS was best achieved by adding 1 mM isopropyl β -D-1-thiogalactopyranoside isopropyl β -d-1-thiogalactopyranoside (IPTG) (Sigma) and incubated 12 h at 20°C. Purification of the N-terminal-10xHis-tagged recombinants JsTPS02 and JsTPS04 were carried out by using a Ni-NTA column kit (Sangon, Shanghai, China), with an elution buffer containing up to 500 mM imidazole.

All constructs were verified by sequencing, and protein concentration after purification was monitored via the Quick Start Bradford protein assay kits using bovine serum albumin as a standard (Bio-Rad). The expected size of the recombinant fusion proteins was checked by SDS-PAGE.

The *in vitro* enzymatic assay was performed in a final volume of 250 μ L consisted of 30 mM HEPES (pH 7.4), 10 mM MgCl₂, 100 mM KCl, 5 mM dithiothreitol, 10% glycerol and 20 μ g of the recombinant protein, together with a substrate either FPP (Sigma-Aldrich, cat. Nr. F6892-1VL) or GPP (Sigma-Aldrich, cat. Nr. G6772-1VL) or GGPP (Sigma-Aldrich, cat. Nr. G6025 -1VL) up to 0.2 mM concentration. After mixing gently, the reaction was carefully overlaid with 250 μ L hexane (cat.nr. 1.04391.4008, Merck KGaA, Darmstadt, Germany) to trap volatile products. The tube was then sealed with parafilm and incubated at 30 °C for 1 h. The reaction was terminated by vortex for 1 min, and then immediately centrifuged at 1200 x g for 30 min at 4°C. The hexane upper layer was transferred into a 2 ml glass vial for GC-MS analysis. As a negative control, heat-inactivated recombinant protein was added to the enzyme assay. Reactions were performed over a range of substrate concentrations from 0 to 300 μ M to determine the substrate-dependent kinetics. Nonlinear regression fitting of the Michaelis-Menten equation was carried out via the GraphPad Prism ver. 8.3.0.

Yeast Microsome Isolation and in vitro enzyme assay of JsTPS01 and JsTPS03

For yeast microsome isolation, culture cells at log phase with an OD_{600nm} of 0.6-0.8 were collected and chilled on ice. Cell pellet after centrifugation at $3,000 \times g$ for 5 min at $4^{\circ}C$ was washed once with half volume of chilled extraction buffer (20 mM Tris-HCl, 10 mM $MgCl_2$, 1 mM EDTA, 5% Glycerol, 1 mM DTT, 1 mM PMSF, pH 8), and re-suspended in residue extraction buffer ($\sim 100 \mu L$). To this, $1 \mu L$ of 0.1M PMSF, $10 \mu L$ freshly prepared protease inhibitors (1 tablet in 1 ml H_2O) and equal volume of acid-washed glass beads (cat. Nr. G8772-500G from Sigma-Aldrich Chemie GmbH, Munich, Germany) were added before performing cell disruption by vortex for 5-10 min in a cold-room. Supernatants after centrifugation at $500 \times g$ for 5 min was combined with that of a second extract of the cell debris by re-suspended in $100 \mu L$ of extraction buffer, $1 \mu L$ of 0.1M PMSF and $10 \mu L$ protease inhibitors, vortex twice for 30 sec and centrifuge again. The microsomal fraction was isolated from the merged supernatants by centrifugation at $100,000 \times g$ for 45 min at $4^{\circ}C$. The microsome pellet was re-suspend in $100 \mu L$ of storage buffer (20 mM Tris-Cl, 0.1 mM EDTA, 10% glycerol, 100mM KCl, 1 mM DTT, 1 mM PMSF, pH 7.5) and $20 \mu L$ protease inhibitors. All the purification steps were conducted either in a cool room or on ice. Protein concentration was estimated by the Bradford protein assay (Bio-lab, Shanghai, China, cat. Nr. 5000002) using bovine serum albumin (BSA) as a calibration standard.

The following *in vitro* enzymatic assay was performed as described above.

Gas chromatography-mass spectrometry analysis

GC-MS analysis was conducted in a Perkin Elmer Clarus 680 GC with SQ 8TGC/MS system coupled to a HP-5 MS capillary column (0.25 mm diameter, 30 m length, and $0.25 \mu m$ film thickness).

For headspace volatile compound, The GC program was isothermal at $40^{\circ}C$ for 4 min, then increased at a rate of $10^{\circ}C \text{ min}^{-1}$ to $70^{\circ}C$ for 3 min, and was then further increased at a rate of $1.5^{\circ}C \text{ min}^{-1}$ to $100^{\circ}C$ for 2 min and $14^{\circ}C \text{ min}^{-1}$ to $240^{\circ}C$ for 2 min (total 44 min).

For extract volatile, The GC program was isothermal at $40^{\circ}C$ for 4 min, then increased at a rate of $10^{\circ}C \text{ min}^{-1}$ to $70^{\circ}C$ for 3 min, and was then further increased at a rate of $3^{\circ}C \text{ min}^{-1}$ to $100^{\circ}C$ for 2 min and $5^{\circ}C \text{ min}^{-1}$ to $280^{\circ}C$ for 2 min (total 60 min).

For analysis of emitted volatiles in *N. benthamiana*, yeast expression product, and *in vitro* enzyme assay, The GC program was isothermal at $50^{\circ}C$ for 3 min, then increased at a rate of $6^{\circ}C \text{ min}^{-1}$ to $200^{\circ}C$ for 1 min, and was then further increased at a rate of $20^{\circ}C \text{ min}^{-1}$ to $240^{\circ}C$ for 2 min (total 33 min).

The detector was activated after a 2.5-min solvent delay. Mass spectra were recorded using the scan mode (total ion count, 45-600 amu). To identify in mixture, mass spectra and linear retention index were searched and compared to the NIST 2020 mass spectra library implemented in the Clarus SQ 8T platform, or when possible, authentic standards were used for qualitative confirmation. For internal standard, $5 \text{ ng}/\mu L$ cedrene was added to the injected samples. Authentic standard compounds linalool (cat. Nr. 51782-1ML) and farnesol (cat. Nr. 43348-1ML) were purchased from Sigma-Aldrich, nerolidol (cat. Nr. B20176 -1ML) from Orileaf (YuanYe[®], Shanghai, China).

Statistical Data analysis

When appropriate, one-way ANOVA and pair-wise multiple t-tests on means of the three biological replicates were conducted using the GraphPad Prism software ver. 8.3.0.

3. Results

3.1. Circadian Emission of VOC in Flowers of J. sambac Dominated by Terpenoids

As a typical night-blooming specie, the flowers of *J. sambac* open approximately at dusk and remain open for about 2 days under nature field conditions. The flower senescence normally occurs after 24 hours post anthesis (hpa) that is obvious by gradually developed purple color in petals (Figure 1a). Abscission of the flower occurred at approximately 48 hpa under the control climate room conditions. It is well known that floral scent of *J. sambac* flowers are released mainly during the first 8 hpa at night. In order to gain more detailed profiles of the floral scents, we analyzed the head-space emission via gas chromatography-mass spectrometry (GC-MS) by sampling at 2-hours-interval in a

48-h duration (Figure 1b). We found that the total emission reached its maximum at approximately 2-3 hpa followed with fluctuated reduction before the dawn. Low level of scent remained during the next daytime, although variation among single flower existed. The second dark/light cycle showed similar emission pattern but with largely reduced volatiles (Figure 1c). Our results also showed that the most abundant VOCs in the headspace of flowers of the *J. sambac* cv 'shuangban' were linalool, α -farnesene and benzyl acetate, making up to 38.1%, 26.7% and 29.4% of the total VOCs at their maximum, respectively (Figure 1b,c upper panel). The three major headspace constituents were somehow different quantitatively between the cultivar here and the Indian one or other close species [44,45]. In the petal extracts, however, α -farnesene was the most predominated compound, with a maximum content up to 112.6 $\mu\text{g}\cdot\text{g}^{-1}$ FW at 23:00 hour. This was followed by cis-3-Hexenyl benzoate (up to 331.5 $\mu\text{g}\cdot\text{g}^{-1}$ FW at 23:00 hour) and τ -cadinol (up to 52.4 $\mu\text{g}\cdot\text{g}^{-1}$ FW) (Figure 1d and Supplementary Data Set S1). It was also noted that the amount of linalool in the petal extracts was lower than 20 $\mu\text{g}\cdot\text{g}^{-1}$ FW during the whole flowering time (Supplementary Data Set 1). Nevertheless, the major VOCs in Jasminum flowers are mainly derived from terpenoid biosynthesis pathway and, to a lesser extent from the benzenoid pathway. Consistent with previously reported by others [46], the floral scent emission in this species follows a circadian rhythm, but only in the first night is a significant scent release observed (Figure 1c).

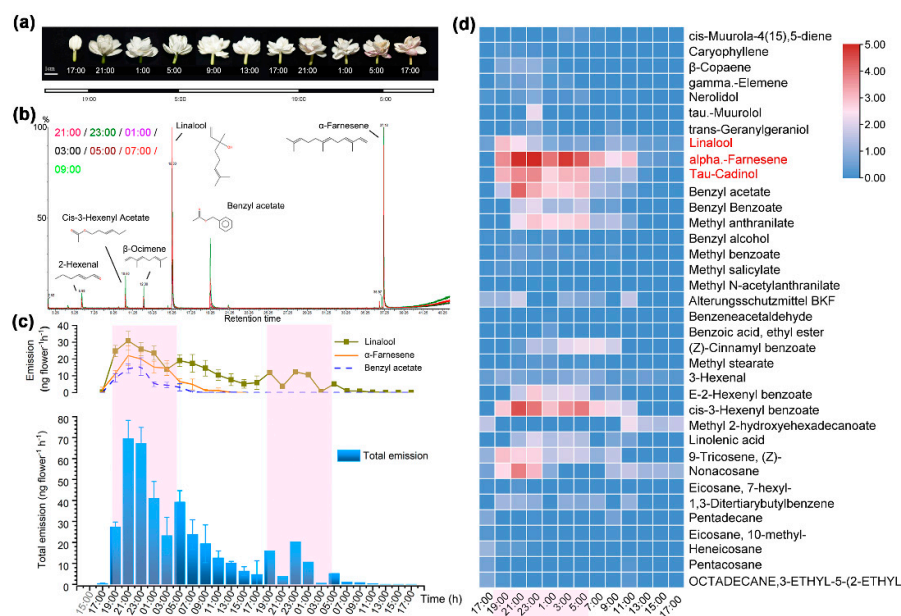


Figure 1. (a) Flowers at various time points post anthesis. The light/dark cycle is indicated below the picture. Scale bar = 1.0 cm; (b) Overlay representative GC-MS spectrum of the headspace VOC during the first 12 h when the emission is maximum; (c) Head-space emission of floral volatiles during 48 h of the flower lifetime; (d) Volatile compounds in petal extracts at time-points during 24 h flower opening.

3.2. Identifying and Cloning of Candidate TPS Genes expressed in Petals

Having characterized the circadian profile of the floral VOCs emission, we sought to isolate the genes corresponding to the biosynthesis of the volatile terpenes. We constructed a transcriptome data set prepared from *Jasminum* flowers, leaves and stem at different time points of day and night. The raw sequence data have been deposited in the Genome Sequence Archive (Genomics, Proteomics & Bioinformatics 2025) in National Genomics Data Center (Nucleic Acids Res 2025), China National Center for Bioinformation/Beijing Institute of Genomics, Chinese Academy of Sciences (GSA: CRA031067) that are publicly accessible at <https://ngdc.cnbc.ac.cn/gsa>. Using BLAST searches against a set of homologous sequences in the transcriptomes followed by manual curation, we identified 34

non-redundant terpene synthase-related genes. Among these genes, 4 genes were highly expressed in flowers, being 2-3 order of magnitudes more abundance in transcript levels comparing with the leaves and stems (Figure 2). Since the transcriptome data represented overall floral tissues other than merely petals that supposed to be the site of VOC synthesis, and was limited in time-point sampling. To profile precisely the expression of these genes in petals, we sampled the flowers at a 2-h-interval during the whole floral life-time (48 h post anthesis) and conducted quantitative measurement using petals RNA isolation. Moreover, the expression patterns of the four putative TPS genes highly correlated with floral terpenoid emission profiles, with maximum mRNA level at the first night (Figure 2b). These four genes *DJ27262*, *DJ12081*, *DJ02562* and *DJ26725*, were assigned as *JsTPS01* (NCBI acc. Nr. MW057924), *JsTPS02* (MW057922), *JsTPS03* (MW057923) and *JsTPS04* (MW057921), respectively. Subsequently the full-length cDNAs were cloned with specific primers (Table S2) and the deduced amino acid sequences showed that they shared 22.26 to 37.80 percent Identities with each other.

Together with other known-function TPS enzymes, a maximum likelihood tree was constructed which revealed that *JsTPS01* belonged to the TPS-a clade while both *JsTPS02* and *JsTPS03* were TPS-b type. The *JsTPS04* was the largest protein among the four, containing 844 amino acid residues with extended N- and C-terminuses, which fell into the TPS-e/f clades of the terpene synthase family (Figure 3a). By TargetP predictions, only *JsTPS02* contained plastid transit peptide, implying a plastidial localization.

In term of sequence similarity, *JsTPS04* is more divergent from the other three terpene synthase enzymes, and its amino acid sequence shares 40.6 and 45.3% identity with the *Clarkia* S-linalool synthase CbLIS (LIS_CLABR) and the *Arabidopsis* geranylinalool synthase TPS04 (Figure 3b). It lacks the N-terminal tandem arginine/tryptophan motif 'RR(x8)W', thought to be critical for monoterpene cyclization [65,66] but also found later [67] in many sesquiterpene and diterpene synthases. *JsTPS04* also contains both the 'DDxxD' and 'NSE/DTE' motifs of metal-binding sites, structural characteristics may distinguish isoprenoid diphosphate lyases and terpenoid cyclases from prenyltransferases [11]. Moreover, the C-terminal domain of *JsTPS04* exists an additional acid motif 'DxxDD', which seems to be a variant form mimicking the general acid motif 'DxDD' signatural in some class II terpenoid synthases [11,24] (Figure 3b). The other three *JsTPS*s all contain the N-terminal 'RRx8W' motif and the typical 'DDxxD', but one of them (*JsTPS01*) has a modified NSE/DTE motif (Figure 3b). Homologous modeling of the protein structures provides an overview of the domain architecture and the conserved Mg²⁺-binding 'DxxDD' motif configuration in the models (Figure S1).

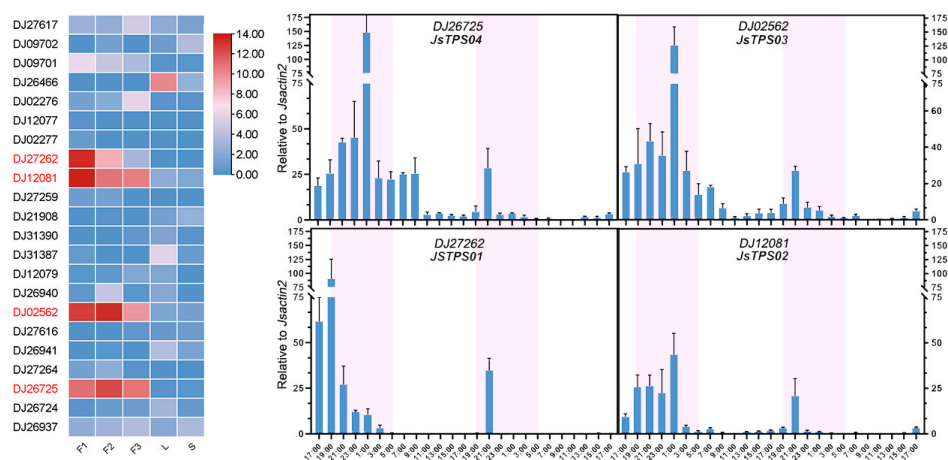


Figure 2. A heatmap depicting the normalized FPKM taken from the transcriptome data and transcript abundance of the most highly expressed *TPS* genes in petals during floral lifetime.

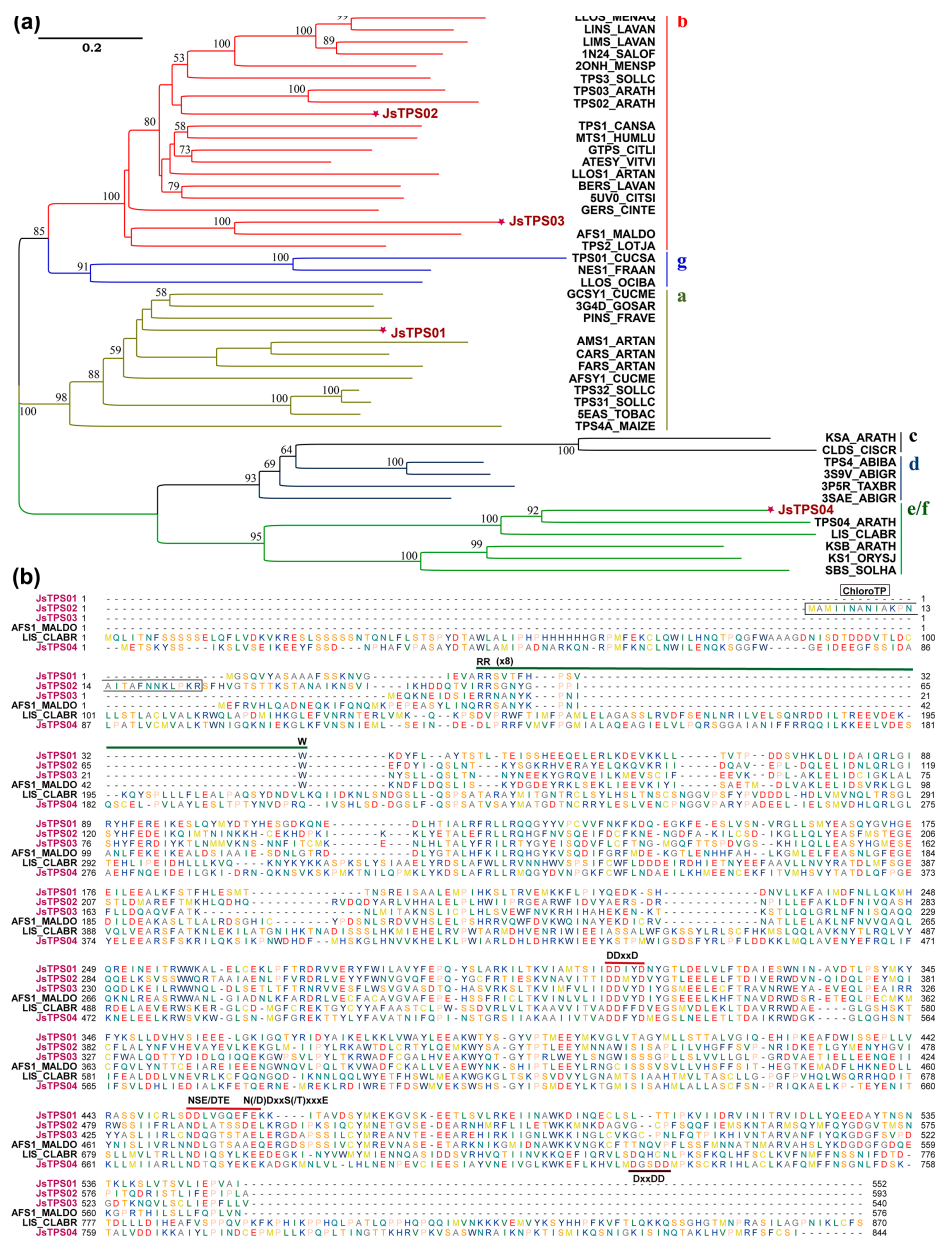


Figure 3. (a) Phylogenetic relationship of JstPSs with other terpene synthases of known function from other species using amino acid sequences (named by SWISS/Pro codes or PDB accession). The tree is constructed using MEGA X ver. ver. 10.1.8 and visualized using FigTree ver. 1.4.4. The scale bar represents amino acid residue substitution rate per site. Subgroups are depicted with color lines and bootstraps values greater than 50 are shown; (b) Amino acid sequence alignment showing the conserved motifs in the JstPS proteins together with those of the (*E,E*)-alpha-farnesene synthase 1 from apple (AFS1_MALDO) and the S-linalol synthase from *Clarkia breweri* (LIS_CLABR). The predicted chloroplast transit peptide in JstPS02 is boxed. The known functional motifs RRX8W, DDXD, NSE/DTE and DDXD are labeled.

3.3. Subcellular Localization of the Four Terpene Synthase Proteins

Since substrates of terpene synthases are mainly derived from the cytosolic MVA and the plastidic MEP pathways, the subcellular localization of a TPS enzyme can be considered a major determinant of its catalytic reaction and also hints for the functionality. Using C-terminal GFP-tagged JstPSs for protoplast transient expression in *Arabidopsis* leaves and *Jasminum* petals, we found that JstPS02 proteins were clearly distributed in the chloroplast or in the plastid-like structures of the petal, consistent with the TargetP prediction, whereas both JstPS01 and JstPS03 enzymes were

mainly cytosolically localized (Figure 4). Interestingly, the fluorescence signal of the JsTPS04-GFP fusion was differently localized between protoplasts of *Arabidopsis* leaves and of *Jasminum* petals. It seemed that JsTPS04 was localized to the cytosol or ER in the leaf protoplasts, but in the petal cells the fluorescence signal was observed in some granular-like structures (Figure 4). A further experiment using *Nicotiana benthamiana* leaf infiltration showed that the JsTPS04-GFP fusion could be localized to both chloroplasts (or particles around the chloroplasts) and cytoplasm in the leaves, while the chloroplast-localization of JsTPS02 and the cytosolic localization of JsTPS01 or JsTPS03 were confirmed, although chloroplast-associated signal were somewhere found irregularly for the latter two (Figure S2).

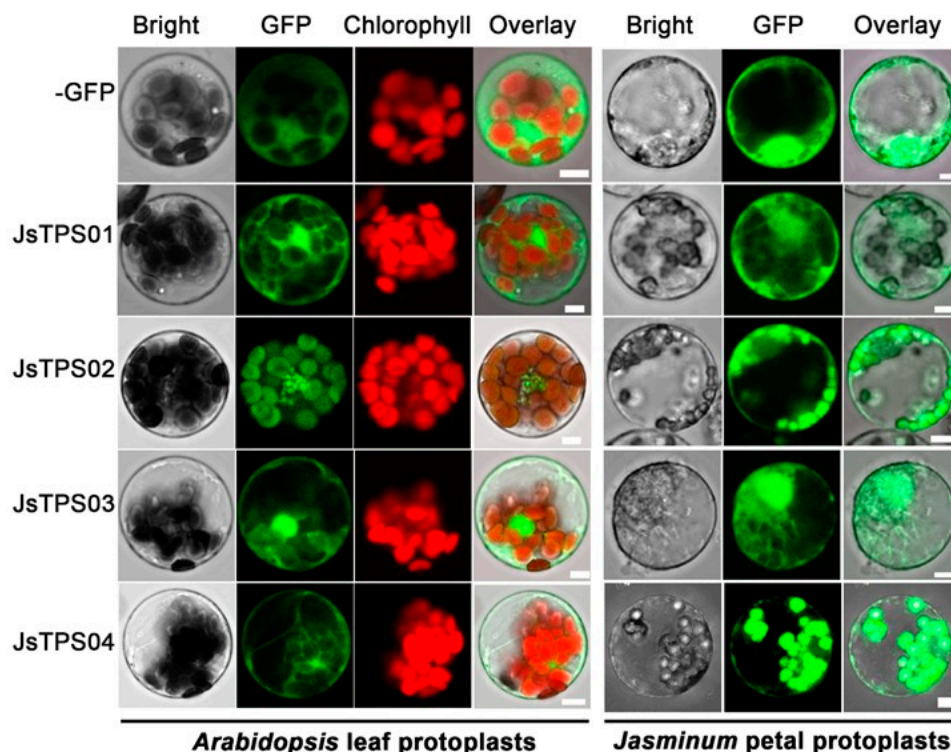


Figure 4. The four JsTPSs in fusion with a C-terminal GFP tag were transiently expressed in protoplasts of *Arabidopsis* rosette leaves or *Jasminum* petals. GFP fluorescence was observed at 470 nm excitation and 525 nm emission; chlorophyll fluorescence at 545 nm excitation and 620 nm emission. Scale bar = 5 μ m.

3.4. Enzyme Activities of the Four *Jasminum* Terpene Synthase Proteins

The *N. benthamiana* leaves transiently expressing the JsTPS-GFP fusions were used for measuring the enzymatic activity. The assay was conducted using leaf extracts with ethyl acetate in a GC-MS system. A significant peak of linalool with a retention time (RT) at 11.67 min was produced in JsTPS04 expressing leaves, whereas the other three TPS did not yield any different peaks within the RT ranges as compared with the GFP alone vector (EV) (Figure 5a). Linalool peak was identified by comparison of the RT and mass spectra with the authentic standard and the NIST20 libraries. We also found that in the EV-transfected leaves, phytol, an acyclic diterpene alcohol and a constituent of chlorophyll, common to green leaves, was the major compound at the C20 range, whilst the expression of the *JsTPSs* induced the accumulation of several aliphatic hydrocarbon and heterocyclic compounds (Figure S3). Some unknown products (RT at ~ 29.1 min) were also induced in JsTPS01/02/03-transfected leaves but absent in the GFP control (EV) and the JsTPS04-expressing leaves. Thus, only the TPS-e/f member JsTPS04 could catalyze the synthesis of linalool when transiently expressed in the *N. benthamiana* leaves. However, they all seemed to interfere with the diterpenoid biosynthesis pathway in the leaves.

In vivo assay for terpenoid accumulation in yeast cell (strain 4742) revealed the significant de novo production of a sesquiterpenoid τ -cadinol in JsTPS01 expressing cells while the other three JsTPSs resulted in no different terpenoid profiles comparing to the empty vector (Figure 5b). Since the yeast cell generally contains less available geranyl diphosphate (GPP) or other prenyl diphosphate but generates a large pool of farnesyl diphosphate (FPP) from the cytosolic mevalonate (MVA) pathway for further synthesis of the sesquiterpene squalene and several essential sterols [68]. Therefore, this endogenous pool of FPP could be used efficiently by JsTPS01 to make τ -cadinol.

We expressed the full-length cDNAs of JsTPSs in *E. coli* to obtain purified recombinant proteins, using a N-terminal fusion of 10xHis-tag. The recombinant 10xHis JsTPS02 and JsTPS04 were readily generated (Figure S4). Although purified recombinant proteins contained His-tag at the N-termina, JsTPS02 show catalytic activities converting the substrates GPP to linalool (Figure 6a), and JsTPS04 converting GPP to linalool, FPP to trans-Nerolidol in a preliminary experiment (Figure 7a). Thus, the recombinant JsTPS02 and JsTPS04 proteins were used in serial reactions with different substrate concentrations to determine the enzymatic property. Using different concentration of GPP (3 μ M, 30 μ M, 45 μ M, 180 μ M, 300 μ M) as substrate, the apparent V_{max} and K_m of the JsTPS02 for substrate GPP were estimated as 47.68 ± 1.68 ng/ μ g $^{-1}$ protein h $^{-1}$ and 28.18 ± 3.42 μ M, respectively (Figure 6 bcd). With varying concentrations of GPP (3 μ M, 9 μ M, 30 μ M, 60 μ M, 90 μ M) as substrate, the apparent V_{max} and K_m of the JsTPS04 for substrate GPP were estimated as 6.20 ± 0.13 ng/ μ g $^{-1}$ protein h $^{-1}$ and 2.51 ± 0.34 μ M, respectively (Figure 7 b,d). Similarly, the apparent V_{max} and K_m of the JsTPS04 for substrate FPP were estimated as 7.57 ± 0.11 ng/ μ g $^{-1}$ protein h $^{-1}$ and 7.58 ± 0.63 μ M, respectively (Figure 7c,d).

Due to unsuccessful expression and purification in *E. coli*, JsTPS01 and JsTPS03 with an N-terminal HA-tag were further expressed in yeast cells. The two JsTPS proteins could be correctly detected as membrane-bound forms by a western blot on isolated total and membrane fractions using an anti-HA antibody (Figure S5). We then isolated the recombinant proteins for an *in vitro* assay using the membrane fractions as enzyme sources. The reactions of JsTPS01 and JsTPS03 did not yield any additional products over the mock control, when using up to 100 μ M GPP as the substrate (Figure 8a). However, JsTPS03 was able to generate farnesol from added FPP at up to 100 μ M, which was not observed for JsTPS01 and the mock control (Figure 8b). The product farnesol was identified by authentic standard comparison (Figure 8c). To characterize the catalytical activities of JsTPS03, we isolated the partially purified proteins and determined the enzymatic kinetics using substrate-dependent assay against FPP concentrations and generated their Michaelis-Menten plots (Figure 8d). The apparent K_m for JsTPS03 was 15.48 ± 3.43 μ M. We were not able to estimate the efficiency parameters of the JsTPS03 due to that the actual concentration of the enzyme molecules were not known in the assay, however, the result should indicate that JsTPS03 were likely to function as farnesene synthases in the *in vitro* assay.

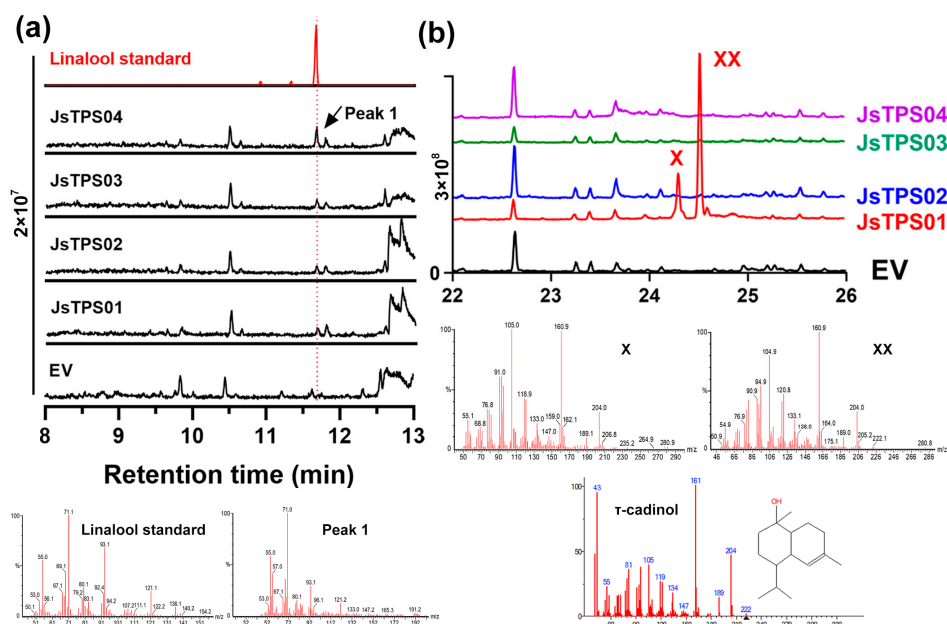


Figure 5. (a) Linalool was produced in *JsTPS04* transfected leaves; (b) A sesquiterpenoid product τ -cadinol was generated in *JsTPS01* expressing yeast cells.

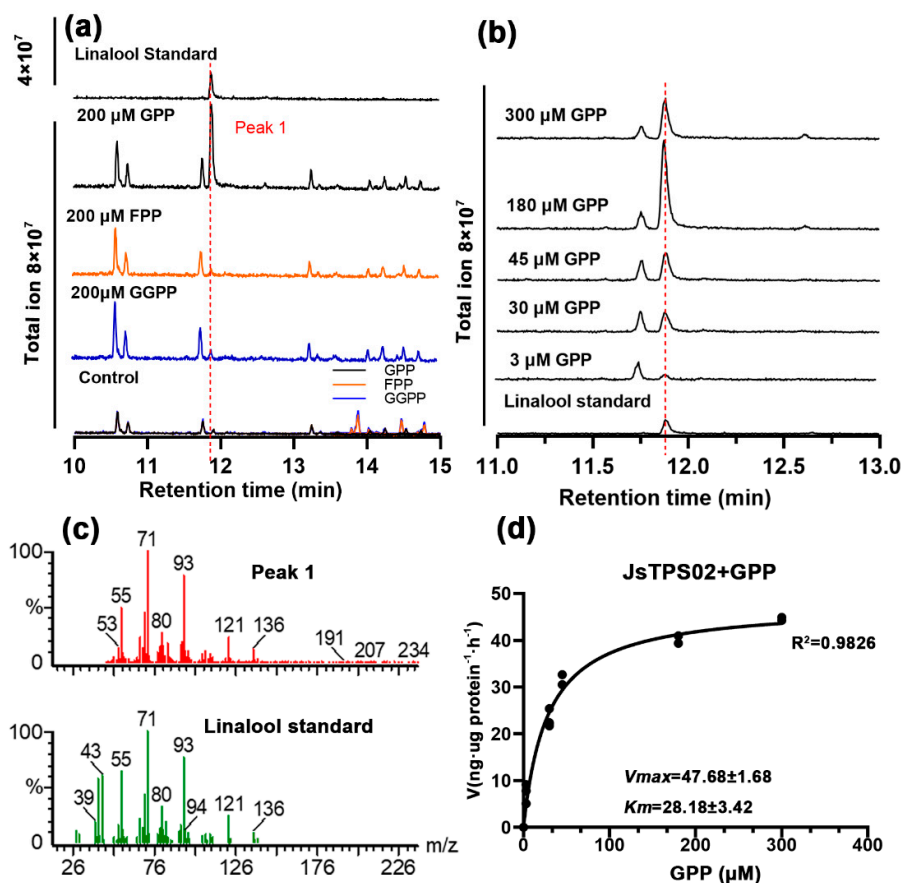


Figure 6. (a) Incubation with GPP, FPP, GGPP up to 200 μ M resulted in linalool; (b) Representative chromatograms of the reaction products; (c) Curve fitting against GPP; (d) Comparison of mass spectrum of the enzymatic product with that of the authentic compound linalool.

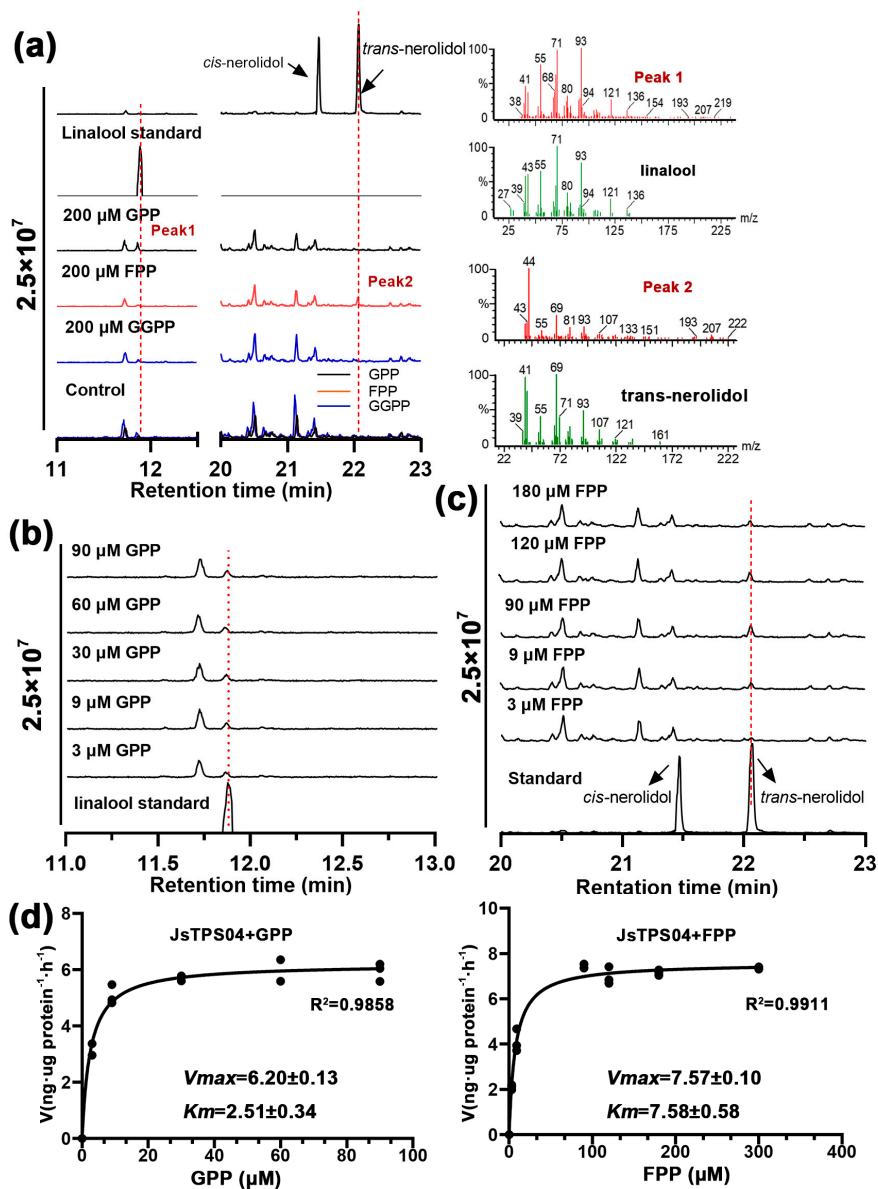


Figure 7. (a) Incubation with GPP, FPP, GGPP up to 200 μM resulted in linalool and trans-nerolidol; (b) Representative chromatograms of the reaction products; (c) Curve fitting against two substrates; (d) Comparison of mass spectrum of the enzymatic product with that of the authentic compound linalool and trans-nerolidol.

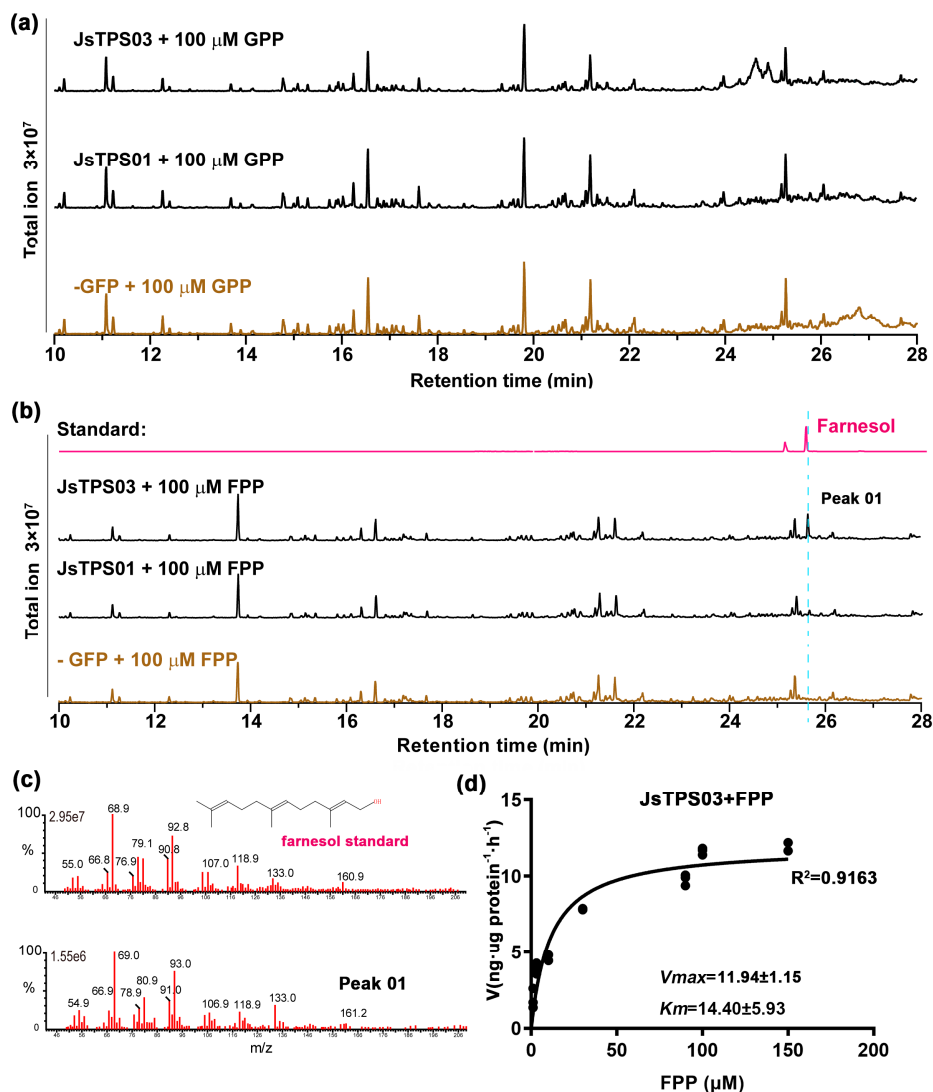


Figure 8. (a) Incubation with GPP up to 100 μM resulted in no significant new product peak; (b) New product corresponding to farnesol was formed by the activity of JsTPS03 using FPP as substrate; (c) Comparison of mass spectrum of the enzymatic product with that of the authentic compound farnesol; (d) Concentration-dependence reaction kinetics of the JsTPS03 against FPP and the apparent Michaelis-Menten parameters.

4. Discussion

In this study, we have identified one monoterpene synthase, two sesquiterpene synthase and one monoterpene/sesquiterpene synthase that responsible for the linalool, farnesol, τ -cadinol, and trans-nerolidol in *J. sambac*, based on their abundant and almost exclusive expression in the petal, as well as on the biochemical characterization in *N. benthamiana* leaves, yeast cell, and *E.coli* cell.

Yeast cells expressing JsTPS01 accumulated τ -cadinol comparing to the empty vector (Figure 5B). Since the yeast cell generally contains less available geranyl diphosphate (GPP) or other prenyl diphosphate but generates a large pool of farnesyl diphosphate (FPP) from the cytosolic mevalonate (MVA) pathway for further synthesis of the sesquiterpene squalene and several essential sterols [68]. Therefore, this endogenous pool of FPP could be used efficiently by JsTPS01 to make τ -cadinol. τ -cadinol is detected in extract of *Jasminum* flowers and was consistently detected throughout the main scent-emission period (Figure 1). So it is possible that JsTPS01 might catalyze the synthesis of τ -cadinol in the flower petal. Since the cadinol family of sesquiterpenoid are known to have

antimicrobial activity [69,70], the expression of JsTPS01 during anthesis might be beneficial for the flower fitness by making sesquiterpenoids involved in defense against microbial pathogens. Quite a few cadinene synthases from other plants have been functionally and structurally determined [11,70–72]. Among them, JsTPS01 has an overall sequence identity of 33.33, 45.78 and 48.05% at the amino acid level with the cadinol synthase LaCADs from *Lavandula angustifolia* [72], (+)-delta-cadinene synthase from *Gossypium arboreum* [71] and cadinene synthase SITPS16 from tomato [25].

The JsTPS02 is a member of the TPS-b clade which may function as a linalool synthase in the *J. sambac* petal. Linalool accounts for the major floral volatile monoterpene in most *J. spp.* fragrance [44] and is a characteristic fragrance constituent of white, night-blooming, moth-pollinated flowers, in addition to many diurnal flowers pollinated by bees, beetles and butterflies [73,74]. JsTPS02 is predicted to contain a signal peptide (Figure 3) and is later correspondingly found in granular structures in the leaf and petal protoplast (Figure 4). Moreover, *in vitro*, JsTPS02 could mediate the biosynthesis of linalool using added GPP as a substrate, with an apparent K_m of $28.18 \pm 3.42 \mu\text{M}$ (Figure 6). Given that JsTPS02 is quite similar to the *Clarkia* S-linalool synthase [75], JsTPS02 might be a linalool synthase. Linalool exists in two different enantiomers in nature: R-(-)-linalool and S-(+)-linalool; while the former is found mostly in woody or leaf essential oils, the latter is emitted from many flowers as the dominant enantiomer [76]. It has been reported that in *J. grandiflorum* flower developmental stages from bud to open flower, an enantiomer ratio shift from R- to S-form occurs with S-(+)-linalool being the most abundance at opening stage [46]. It remains to be determined whether JsTPS02 could produce both or preferentially S-form linalool. In addition, as reported in many natural linalool-emitting plant or transgenic plants over-expressing linalool synthases, linalool glycosides are the major forms for transport and storage before release [35,73,77]. We also showed that the free linalool in the petal extract with hexane was rather low as comparing to the large portion in the headspace (Figure 1d). It could be possible that the *Jasminum* flower may contain similar pool of conjugated nonvolatile linalool in the petal subcellular structures before emission, as showed in a recent study using four *Jasminum* species [47].

JsTPS03 could mediate the biosynthesis of farnesol in isolated membrane fraction from ectopically expressing yeast cells using added FPP as a substrate with an apparent K_m of $15.48 \pm 3.43 \mu\text{M}$ (Figure 8a). JsTPS03 belongs to the TPS-b subfamily, sharing 45.1% with the apple α -farnesene synthase AFS1_MALDO [78]. Most plant sesquiterpene synthases in purified form have a reported FPP affinity ranging from 0.4 to $142.9 \mu\text{M}$, but typically close to around $10 \mu\text{M}$ [79], so we speculate that the JsTPS03 should function as a farnesene synthases in the *Jasminum* petal.

JsTPS04 belongs to the TPS-e/f clade. Its transient expression in *Nicotiana benthamiana* leaves yielded linalool, also the recombinant protein could convert GPP into linalool *in vitro*, implying that JsTPS04 possesses linalool-synthase activity. Both JsTPS02 and JsTPS 04 recombinant protein catalyze the conversion of GPP to linalool, with an apparent K_m of $28.18 \pm 3.42 \mu\text{M}$ and $2.51 \pm 0.34 \mu\text{M}$, respectively (Figures 6a and 7a). It is therefore that the JsTPS04 has a higher affinity to the substrate than JsTPS02 *in vitro*. Moreover, JsTPS04 also accepted FPP to produce tans-nerolidol with an apparent K_m of $7.58 \pm 0.63 \mu\text{M}$, which was detected both in petal extracts and throughout the floral scent-emission period. Thus, we speculate that the JsTPS04 should also function as a nerolidol synthases in the *Jasminum* petal, demonstrating that the enzyme functions as a nerolidol synthase as well. Collectively, these results indicate that JsTPS04 is a bifunctional terpene synthase capable of generating both monoterpenes and sesquiterpenes. This is consistent with its multiple subcellular localizations in. Moreover, in the petal protoplast, JsTPS04 is found in granular structures, however, it can catalyze the conversion of FPP into sesquiterpenes—a phenomenon that has also been reported previously. e.g. The plastic-located farnesene synthase PvHVS from *Prunella vulgaris* (family Lamiaceae), a member of the TPS-a clade, can use FPP to make bisabolol and farnesene *in vitro* [80].

In summary, we identified a linalool synthase (JsTPS02), a cadinol synthase (JsTPS01), and a bifunctional mono-/sesquiterpene synthase (JsTPS04) that produces linalool/tans-nerolidol, and a putative farnesene synthase (JsTPS03) in *J. sambac* petals. Although we could not roll out the existence

of other terpene synthases in the flower, JsTPS04 and JsTPS03 are the best candidate responsible for the synthesis of linalool and farnesene to be released from the petal, respectively.

Supplementary Materials: The following supporting information can be downloaded at the website of this paper posted on Preprints.org, Data S1: List of compounds identified in the headspace and ethyl acetate extracts from petals at various time-points during the flowering lifetime and the quantification; Figure S1: Homologous models of the four JsTPSs showing the conserved Mg²⁺ binding DDxxD motif in each protein structure. The models are built via SWISS-MODEL homology-modelling server (<https://swissmodel.expasy.org/>). Magnesium ion is depicted as green ball, and the aspartates side chains at the conserved Mg²⁺ binding motif, as well as at the acid motif, are showed as sticks; Figure S2: Representative images of transient expression of GFP-tagged TPS proteins in leaves of *Nicotiana benthamiana*; Figure S3: JsTPSs induced the accumulation of several aliphatic hydrocarbon and heterocyclic compounds in *N. benthamiana* leaves transiently expressing TPS genes; Figure S4: Production of JsTPS02 and JsTPS04 recombinant proteins in *E. coli*. Proteins were separated on 10% SDS-PAGE and the gel was stained with 1.25% Coomassie Blue R250. A: Induction and Western blot detection of the four JsTPS recombinant proteins; B: Purification of the four JsTPS recombinant proteins; Figure S5: JsTPS01 and JsTPS03 expression in yeast were detected with an antibody against the N-terminal HA-tag. EV, empty vector; W, whole cell lysates; M, membrane fraction. 15 μ l of sample was loaded in each lane.; Table S1: Four JsTPSs from Jasminum flower/leaf transcriptomes and the respective qRT-PCR primers used; Table S2: List of primer sequences used in CDS cloning and vector constructions.

Author Contributions: Conceived and designed the research, B.W. and Y.Y.; experimental validation, Y.Y., X.H. and L.H.; data analysis, Y.W., C.W., Y.Z., W.W., and J.L.; visualization, Y.Y. and B.W.; writing—original draft preparation, B.W. and Y.Y. All authors have read and agreed to the published version of the manuscript.

Funding: This research was funded by Fujian Natural Science Foundation, grant number Nr. 2022J01588, National Natural Science Foundation of China, grant number Nr. 31902050 and Fujian Agriculture and Forestry University Special Fund for Scientific and Technological Innovation, grant number Nr. KFB23033 from Y.Y.

Data Availability Statement: All data supporting the findings of this study are available within the paper and within its supplementary materials published online. Further information may be obtained from the corresponding author, B. Wu.

Acknowledgments: We thank Ms. Lingjuan Huang for excellent technical assistances.

Conflicts of Interest: All authors state no conflict of interest concerning this manuscript.

References

1. Pichersky, E. and Lewinsohn, E., Convergent Evolution in Plant Specialized Metabolism. *Annual Review of Plant Biology* 2011. 62,549-566.
2. Mithöfer, A. and Boland, W., Plant Defense Against Herbivores: Chemical Aspects. *Annual Review of Plant Biology* 2012. 63,431-450.
3. Booi-James, I.S., Dube, S.K., Jansen, M.A., Edelman, M., and Mattoo, A.K., Ultraviolet-B radiation impacts light-mediated turnover of the photosystem II reaction center heterodimer in Arabidopsis mutants altered in phenolic metabolism. *Plant Physiol* 2000. 124(3),1275-84.
4. Knudsen, J.T., Tollsten, L., and Bergström, L.G., Floral scents—a checklist of volatile compounds isolated by head-space techniques. *Phytochemistry* 1993. 33(2),253-280.
5. Amrad, A., Moser, M., Mandel, T., de Vries, M., Schuurink, R.C., Freitas, L., and Kuhlemeier, C., Gain and Loss of Floral Scent Production through Changes in Structural Genes during Pollinator-Mediated Speciation. *Curr Biol* 2016. 26(24),3303-3312.
6. Dixon, R.A. and Strack, D., Phytochemistry meets genome analysis, and beyond. *Phytochemistry* 2003. 62(6),815-6.
7. Milo, R. and Last, R.L., Achieving Diversity in the Face of Constraints: Lessons from Metabolism. *Science* 2012. 336(6089),1663-1667.

8. Weng, J.-K., Philippe, R.N., and Noel, J.P., The Rise of Chemodiversity in Plants. *Science* 2012. 336(6089),1667-1670.
9. Leong, B.J. and Last, R.L., Promiscuity, impersonation and accommodation: evolution of plant specialized metabolism. *Current Opinion in Structural Biology* 2017. 47,105-112.
10. Gao, Y., Honzatko, R.B., and Peters, R.J., Terpenoid synthase structures: a so far incomplete view of complex catalysis. *Natural Product Reports* 2012. 29(10),1153-1175.
11. Christianson, D.W., Structural and Chemical Biology of Terpenoid Cyclases. *Chem Rev* 2017. 117(17),11570-11648.
12. Takahashi, S. and Koyama, T., Structure and function of cis-prenyl chain elongating enzymes. *The Chemical Record* 2006. 6(4),194-205.
13. Hemmerlin, A., Harwood, J.L., and Bach, T.J., A raison d'être for two distinct pathways in the early steps of plant isoprenoid biosynthesis? *Progress in Lipid Research* 2012. 51(2),95-148.
14. Liang, P.-H., Ko, T.-P., and Wang, A.H.J., Structure, mechanism and function of prenyltransferases. *European journal of biochemistry* 2002. 269(14),3339-3354.
15. Kharel, Y. and Koyama, T., Molecular Analysis of cis-Prenyl Chain Elongating Enzymes. *ChemInform* 2003. 34(17).
16. Hamberger, B. and Bak, S., Plant P450s as versatile drivers for evolution of species-specific chemical diversity. *Philosophical Transactions of the Royal Society B: Biological Sciences* 2013. 368(1612),20120426.
17. Banerjee, A. and Hamberger, B., P450s controlling metabolic bifurcations in plant terpene specialized metabolism. *Phytochem Rev* 2018. 17(1),81-111.
18. Karunanithi, P.S. and Zerbe, P., Terpene Synthases as Metabolic Gatekeepers in the Evolution of Plant Terpenoid Chemical Diversity. *Frontiers in Plant Science* 2019. Volume 10 - 2019.
19. Pichersky, E. and Gershenzon, J., The formation and function of plant volatiles: perfumes for pollinator attraction and defense. *Current Opinion in Plant Biology* 2002. 5(3),237-243.
20. Magnard, J.-L., Rocchia, A., Caissard, J.-C., Vergne, P., Sun, P., Hecquet, R., Dubois, A., Hibrand-Saint Oyant, L., Jullien, F., Nicolè, F., Raymond, O., Huguet, S., Baltenweck, R., Meyer, S., Claudel, P., Jeauffre, J., Rohmer, M., Foucher, F., Hugueney, P., Bendahmane, M., and Baudino, S., Biosynthesis of monoterpene scent compounds in roses. *Science* 2015. 349(6243),81-83.
21. Boutanaev, A.M., Moses, T., Zi, J., Nelson, D.R., Mugford, S.T., Peters, R.J., and Osbourn, A., Investigation of terpene diversification across multiple sequenced plant genomes. *Proc Natl Acad Sci U S A* 2015. 112(1),E81-8.
22. Beran, F., Rahfeld, P., Luck, K., Nagel, R., Vogel, H., Wielsch, N., Irmisch, S., Ramasamy, S., Gershenzon, J., Heckel, D.G., and Köllner, T.G., Novel family of terpene synthases evolved from *trans*-isoprenyl diphosphate synthases in a flea beetle. *Proceedings of the National Academy of Sciences* 2016. 113(11),2922-2927.
23. Jia, Q., Li, G., Köllner, T.G., Fu, J., Chen, X., Xiong, W., Crandall-Stotler, B.J., Bowman, J.L., Weston, D.J., Zhang, Y., Chen, L., Xie, Y., Li, F.-W., Rothfels, C.J., Larsson, A., Graham, S.W., Stevenson, D.W., Wong, G.K.-S., Gershenzon, J., and Chen, F., Microbial-type terpene synthase genes occur widely in nonseed land plants, but not in seed plants. *Proceedings of the National Academy of Sciences* 2016. 113(43),12328-12333.
24. Alicandri, E., Paolacci, A.R., Osadolor, S., Sorgonà, A., Badiani, M., and Ciaffi, M., On the Evolution and Functional Diversity of Terpene Synthases in the Pinus Species: A Review. *J Mol Evol* 2020. 88(3),253-283.
25. Zhou, F. and Pichersky, E., The complete functional characterisation of the terpene synthase family in tomato. *New Phytologist* 2020. 226(5),1341-1360.
26. Dudareva, N., & Pichersky, E, *Biology of Floral Scent*. 1st Edition ed. 2006, Boca Raton: CRC Press.
27. Dudareva, N., Klempien, A., Muhlemann, J.K., and Kaplan, I., Biosynthesis, function and metabolic engineering of plant volatile organic compounds. *New Phytol* 2013. 198(1),16-32.
28. Schiestl, F.P., Ecology and evolution of floral volatile-mediated information transfer in plants. *New Phytologist* 2015. 206(2),571-577.
29. Sas, C., Müller, F., Kappel, C., Kent, T.V., Wright, S.I., Hilker, M., and Lenhard, M., Repeated Inactivation of the First Committed Enzyme Underlies the Loss of Benzaldehyde Emission after the Selfing Transition in *Capsella*. *Current Biology* 2016. 26(24),3313-3319.

30. Chen, F., Tholl, D., D'Auria, J.C., Farooq, A., Pichersky, E., and Gershenzon, J., Biosynthesis and emission of terpenoid volatiles from Arabidopsis flowers. *Plant Cell* 2003. 15(2),481-94.
31. Tholl, D. and Lee, S., Terpene Specialized Metabolism in Arabidopsis thaliana. *The Arabidopsis book / American Society of Plant Biologists* 2011. 9,e0143.
32. Tholl, D., Chen, F., Petri, J., Gershenzon, J., and Pichersky, E., Two sesquiterpene synthases are responsible for the complex mixture of sesquiterpenes emitted from Arabidopsis flowers. *The Plant Journal* 2005. 42(5),757-771.
33. Falara, V., Akhtar, T.A., Nguyen, T.T.H., Spyropoulou, E.A., Bleeker, P.M., Schauvinhold, I., Matsuba, Y., Bonini, M.E., Schillmiller, A.L., Last, R.L., Schuurink, R.C., and Pichersky, E., The Tomato Terpene Synthase Gene Family. *Plant Physiology* 2011. 157(2),770-789.
34. Dudareva, N., Raguso, R.A., Wang, J., Ross, J.R., and Pichersky, E., Floral scent production in *Clarkia breweri*. III. Enzymatic synthesis and emission of benzenoid esters. *Plant Physiol* 1998. 116(2),599-604.
35. Lückner, J., Bouwmeester, H.J., Schwab, W., Blaas, J., Van Der Plas, L.H.W., and Verhoeven, H.A., Expression of *Clarkia* S-linalool synthase in transgenic petunia plants results in the accumulation of S-linalyl- β -D-glucopyranoside. *The Plant Journal* 2001. 27(4),315-324.
36. Tholl, D., Kish, C.M., Orlova, I., Sherman, D., Gershenzon, J., Pichersky, E., and Dudareva, N., Formation of Monoterpenes in *Antirrhinum majus* and *Clarkia breweri* Flowers Involves Heterodimeric Geranyl Diphosphate Synthases. *The Plant Cell* 2004. 16(4),977-992.
37. Weiss, J., Mühlemann, J.K., Ruiz-Hernández, V., Dudareva, N., and Egea-Cortines, M., Phenotypic Space and Variation of Floral Scent Profiles during Late Flower Development in *Antirrhinum*. *Frontiers in Plant Science* 2016. Volume 7 - 2016.
38. Xu, H., Bohman, B., Wong, D.C.J., Rodriguez-Delgado, C., Scaffidi, A., Flematti, G.R., Phillips, R.D., Pichersky, E., and Peakall, R., Complex Sexual Deception in an Orchid Is Achieved by Co-opting Two Independent Biosynthetic Pathways for Pollinator Attraction. *Current Biology* 2017. 27(13),1867-1877.e5.
39. Chuang, Y.C., Hung, Y.C., Tsai, W.C., Chen, W.H., and Chen, H.H., PbbHLH4 regulates floral monoterpene biosynthesis in *Phalaenopsis* orchids. *J Exp Bot* 2018. 69(18),4363-4377.
40. Ramya, M., Jang, S., An, H.-R., Lee, S.-Y., Park, P.-M., and Park, P.H., Volatile Organic Compounds from Orchids: From Synthesis and Function to Gene Regulation. *International Journal of Molecular Sciences* 2020. 21(3),1160.
41. Pichersky, E. and Raguso, R.A., Why do plants produce so many terpenoid compounds? *New Phytologist* 2018. 220(3),692-702.
42. Thompson, J.D. and Dommée, B., Sequential variation in the components of reproductive success in the distylous *Jasminum fruticans* (Oleaceae). *Oecologia* 1993. 94(4),480-487.
43. QixiangYu, LixinRu, ChenshuangShuang, Fengjing, Chenhuijie, LiuxinTong, JinyuYan, and DengyanMing, Identification of the FLA Gene Family and Functional Analysis of JsFLA2 in *Jasminum sambac*. *Scientia Agricultura Sinica* 2025. 58(17),3516-3530.
44. Bera, P., Kotamreddy, J.N., Samanta, T., Maiti, S., and Mitra, A., Inter-specific variation in headspace scent volatiles composition of four commercially cultivated jasmine flowers. *Nat Prod Res* 2015. 29(14),1328-35.
45. Bera, P., Mukherjee, C., and Mitra, A., Enzymatic production and emission of floral scent volatiles in *Jasminum sambac*. *Plant Science* 2017. 256,25-38.
46. Pragadheesh, V.S., Chanotiya, C.S., Rastogi, S., and Shasany, A.K., Scent from *Jasminum grandiflorum* flowers: Investigation of the change in linalool enantiomers at various developmental stages using chemical and molecular methods. *Phytochemistry* 2017. 140,83-94.
47. Barman, M. and Mitra, A., Temporal relationship between emitted and endogenous floral scent volatiles in summer- and winter-blooming *Jasminum* species. *Physiologia Plantarum* 2019. 166(4),946-959.
48. Chen, G., Mostafa, S., Lu, Z., Du, R., Cui, J., Wang, Y., Liao, Q., Lu, J., Mao, X., Chang, B., Gan, Q., Wang, L., Jia, Z., Yang, X., Zhu, Y., Yan, J., and Jin, B., The Jasmine (*Jasminum sambac*) Genome Provides Insight into the Biosynthesis of Flower Fragrances and Jasmonates. *Genomics, Proteomics & Bioinformatics* 2023. 21(1),127-149.

49. Qi, X., Wang, H., Liu, S., Chen, S., Feng, J., Chen, H., Qin, Z., Chen, Q., Blilou, I., and Deng, Y., The chromosome-level genome of double-petal phenotype jasmine provides insights into the biosynthesis of floral scent. *Horticultural Plant Journal* 2024. 10(1),259-272.
50. Fan, W., Liao, Z., Gu, M., Zhang, Y., Lei, W., Zhang, Y., Li, H., Yan, J., Xiao, Y., Lin, H., Jin, S., Yu, Y., Fang, J., Ye, N., and Wang, P., Pan-Genome of *Jasminum sambac* Reveals the Genetic Diversity of Different Petal Morphology and Aroma-Related Genes. *Mol Ecol Resour* 2025. 25(7),e70013.
51. Qi, X., Wang, H., Chen, S., Feng, J., Chen, H., Qin, Z., Blilou, I., and Deng, Y., The genome of single-petal jasmine (*Jasminum sambac*) provides insights into heat stress tolerance and aroma compound biosynthesis. *Frontiers in Plant Science* 2022. Volume 13 - 2022.
52. Xu, S., Ding, Y., Sun, J., Zhang, Z., Wu, Z., Yang, T., Shen, F., and Xue, G., A high-quality genome assembly of *Jasminum sambac* provides insight into floral trait formation and Oleaceae genome evolution. *Molecular Ecology Resources* 2022. 22(2),724-739.
53. Wang, P., Fang, J., Lin, H., Yang, W., Yu, J., Hong, Y., Jiang, M., Gu, M., Chen, Q., Zheng, Y., Liao, Z., Chen, G., Yang, J., Jin, S., Zhang, X., and Ye, N., Genomes of single- and double-petal jasmines (*Jasminum sambac*) provide insights into their divergence time and structural variations. *Plant Biotechnol J* 2022. 20(7),1232-1234.
54. Chen, G., Mostafa, S., Lu, Z., Du, R., Cui, J., Wang, Y., Liao, Q., Lu, J., Mao, X., Chang, B., Wang, L., Jia, Z., Yang, X., Zhu, Y., Yan, J., and Jin, B., The jasmine (*Jasminum sambac*) genome and flower fragrances. *bioRxiv* 2020.
55. Hong Ya-ping, Chen Xue-jin, Wang Peng-jie, GU Meng-ya, GAO Ting, YE Nai-xing. Transcriptome Identification of Terpenoid Synthase Genes in *Jasminum sambac* and Their Expressions Responding to Exogenous Hormones[J]. *Biotechnology Bulletin*, 2022, 38(3): 41-49.
56. Kim, D., Langmead, B., and Salzberg, S.L., HISAT: a fast spliced aligner with low memory requirements. *Nat Methods* 2015. 12(4),357-60.
57. Wu, T., Hu, E., Xu, S., Chen, M., Guo, P., Dai, Z., Feng, T., Zhou, L., Tang, W., Zhan, L., Fu, X., Liu, S., Bo, X., and Yu, G., clusterProfiler 4.0: A universal enrichment tool for interpreting omics data. *The Innovation* 2021. 2(3),100141.
58. Karimi, M., Inze, D., and Depicker, A., GATEWAY vectors for Agrobacterium-mediated plant transformation. *Trends in plant science* 2002. 7(5),193-5.
59. Lu, Y., Liu, Z., Lyu, M., Yuan, Y., and Wu, B., Characterization of JsWOX1 and JsWOX4 during Callus and Root Induction in the Shrub Species *Jasminum sambac*. *Plants (Basel, Switzerland)* 2019. 8(4).
60. Kumar, S., Stecher, G., Li, M., Knyaz, C., and Tamura, K., MEGA X: Molecular Evolutionary Genetics Analysis across Computing Platforms. *Molecular Biology and Evolution* 2018. 35(6),1547-1549.
61. Schmittgen, T.D. and Livak, K.J., Analyzing real-time PCR data by the comparative CT method. *Nature Protocols* 2008. 3(6),1101-1108.
62. Wang, P., Wei, P., Niu, F., Liu, X., Zhang, H., Lyu, M., Yuan, Y., and wu, B., Cloning and Functional Assessments of Floral-Expressed SWEET Transporter Genes from *Jasminum sambac*. *International Journal of Molecular Sciences* 2019. 20,4001.
63. Wu, B., Rambow, J., Bock, S., Holm-Bertelsen, J., Wiechert, M., Soares, A.B., Spielmann, T., and Beitz, E., Identity of a Plasmodium lactate/H⁺ symporter structurally unrelated to human transporters. *Nature Communications* 2015. 6(1),6284.
64. Gietz, R.D. and Schiestl, R.H., High-efficiency yeast transformation using the LiAc/SS carrier DNA/PEG method. *Nat Protoc* 2007. 2(1),31-4.
65. Whittington, D.A., Wise, M.L., Urbansky, M., Coates, R.M., Croteau, R.B., and Christianson, D.W., Bornyl diphosphate synthase: Structure and strategy for carbocation manipulation by a terpenoid cyclase. *Proceedings of the National Academy of Sciences* 2002. 99(24),15375-15380.
66. Hyatt, D.C., Youn, B., Zhao, Y., Santhamma, B., Coates, R.M., Croteau, R.B., and Kang, C., Structure of limonene synthase, a simple model for terpenoid cyclase catalysis. *Proceedings of the National Academy of Sciences* 2007. 104(13),5360-5365.

67. Jiang, S.-Y., Jin, J., Sarojam, R., and Ramachandran, S., A Comprehensive Survey on the Terpene Synthase Gene Family Provides New Insight into Its Evolutionary Patterns. *Genome Biology and Evolution* 2019. 11(8),2078-2098.
68. Fujii, T., Nagasawa, N., Iwamatsu, A., Bogaki, T., Tamai, Y., and Hamachi, M., Molecular cloning, sequence analysis, and expression of the yeast alcohol acetyltransferase gene. *Applied and Environmental Microbiology* 1994. 60(8),2786-2792.
69. Cheng, S.S., Wu, C.L., Chang, H.T., Kao, Y.T., and Chang, S.T., Antitermitic and antifungal activities of essential oil of *Calocedrus formosana* leaf and its composition. *J Chem Ecol* 2004. 30(10),1957-67.
70. Ren, F., Mao, H., Liang, J., Liu, J., Shu, K., and Wang, Q., Functional characterization of ZmTPS7 reveals a maize τ -cadinol synthase involved in stress response. *Planta* 2016. 244(5),1065-1074.
71. Gennadios, H.A., Gonzalez, V., Costanzo, L.D., Li, A., and Christianson, D.W., Crystal Structure of (+)- δ -Cadinene Synthase from *Gossypium arboreum* and Evolutionary Divergence of Metal Binding Motifs for Catalysis. *Biochemistry* 2009. 48(26),6175-6183.
72. Jullien, F., Moja, S., Bony, A., Legrand, S., Petit, C., Benabdelkader, T., Poirot, K., Fiorucci, S., Guitton, Y., Nicolè, F., Baudino, S., and Magnard, J.-L., Isolation and functional characterization of a τ -cadinol synthase, a new sesquiterpene synthase from *Lavandula angustifolia*. *Plant Molecular Biology* 2014. 84(1),227-241.
73. Raguso, R.A. and Pichersky, E., New Perspectives in Pollination Biology: Floral Fragrances. A day in the life of a linalool molecule: Chemical communication in a plant-pollinator system. Part 1: Linalool biosynthesis in flowering plants. *Plant Species Biology* 1999. 14(2),95-120.
74. Farré-Armengol, G., Fernández-Martínez, M., Filella, I., Junker, R.R., and Peñuelas, J., Deciphering the Biotic and Climatic Factors That Influence Floral Scents: A Systematic Review of Floral Volatile Emissions. *Frontiers in Plant Science* 2020. Volume 11 - 2020.
75. Dudareva, N., Cseke, L., Blanc, V.M., and Pichersky, E., Evolution of floral scent in *Clarkia*: novel patterns of S-linalool synthase gene expression in the *C. breweri* flower. *Plant Cell* 1996. 8(7),1137-48.
76. Aprotosoiaie, A.C., Hăncianu, M., Costache, I.-I., and Miron, A., Linalool: a review on a key odorant molecule with valuable biological properties. *Flavour and Fragrance Journal* 2014. 29(4),193-219.
77. Yang, T., Stoopen, G., Thoen, M., Wieggers, G., and Jongsma, M.A., *Chrysanthemum* expressing a linalool synthase gene 'smells good', but 'tastes bad' to western flower thrips. *Plant Biotechnology Journal* 2013. 11(7),875-882.
78. Green, S., Friel, E.N., Matich, A., Beuning, L.L., Cooney, J.M., Rowan, D.D., and MacRae, E., Unusual features of a recombinant apple α -farnesene synthase. *Phytochemistry* 2007. 68(2),176-188.
79. Manczak, T. and Simonsen, H.T., Insight into Biochemical Characterization of Plant Sesquiterpene Synthases. *Anal Chem Insights* 2016. 11(Suppl 1),1-7.
80. Johnson, S.R., Bhat, W.W., Sadre, R., Miller, G.P., Garcia, A.S., and Hamberger, B., Promiscuous terpene synthases from *Prunella vulgaris* highlight the importance of substrate and compartment switching in terpene synthase evolution. *New Phytologist* 2019. 223(1),323-335.

Disclaimer/Publisher's Note: The statements, opinions and data contained in all publications are solely those of the individual author(s) and contributor(s) and not of MDPI and/or the editor(s). MDPI and/or the editor(s) disclaim responsibility for any injury to people or property resulting from any ideas, methods, instructions or products referred to in the content.